Supporting Online Material for

Network Analysis of Oncogenic Ras Activation in Cancer

Edward C. Stites, Paul C. Trampont, Zhong Ma, Kodi S. Ravichandran*

*To whom correspondence should be addressed. E-mail: Ravi@virginia.edu

Published 19 October 2007, *Science* **318**, 243 (2007)
DOI: 10.1126/science1144642

This PDF file includes

I. MATERIALS AND METHODS:

Phospho-ERK analysis by flow cytometry.

HEK-293T cells were transiently transfected using calcium phosphate (Promega) with 3×HA-tagged N-Ras^{G12V} or 3×HA-tagged N-Ras^{F28L}. For each experiment, we used 0.2, 0.6, 2, and 6 μg of DNA per 60 mm plate. 36 hours after transfection, 293T cells were harvested and immediately fixed for 10 minutes at room temperature in PBS containing 2% paraformaldehyde (PFA, Electron microscopy Services, PA). Cells were then permeabilized in 90% methanol at 4ºC for one hour, washed twice in cold PBS (containing protease and phosphatase inhibitors) to remove the methanol, and resuspended in phospho-buffer (PBS, 0.5%BSA, 0.05%NaN3 plus protease and phosphatase inhibitors) for rehydration. After centrifugation, 0.05 μg of antibody per well in 100μl of antibody mix for an alexa-647 conjugated phospho-ERK antibody (anti phospho-p44/42 MAP Kinase,Thr202/Tyr204, Cell Signaling) and for an alexa-488 conjugated anti-HA tag antibody (anti HA Tag (6E2) mouse mAb, Cell Signaling) was added and incubated for one hour at 4ºC. Cells were analyzed by flow cytometry on a BD Facs Canto cytometer using DIVA software.

Ras activation assay

Ras activation was assessed in cell lines with (T24, HT1080, MDA-MB-231) or without (HeLa, HEK-293T) described oncogenic Ras point mutants using bacterially produced GST-RBD as previously described *(S1)*. 750 μL of the whole cell lysate was used for the RBD assay. 50 μL of the whole cell lysates was saved for Western blotting. Equal amounts of total protein were loaded in parallel on a 12% SDS-PAGE gel. Nitrocellulose membranes were probed with antibodies for H-Ras (Santa Cruz Biotechnology), N-Ras (Santa Cruz Biotechnology), K-Ras (Sigma), pan-Ras (Calbiochem), or ERK2 (Santa Cruz Biotechnology). Densitometry of the Western Blot was performed using Image Quant 5.2 software.

Generation of the model

The reactions of the module (Fig. 1A) were described with mass action kinetics:

R1) Rate of free GDP exchange = $k_{d,GDP}[Ras_{GDP}] - k_{a,GDP}[Ras_{nt\ free}][GDP]$

R2) Rate of free GTP exchange = $k_{d,GTP}[Ras_{GTP}] - k_{a,GTP}[Ras_{nt\ free}][GTP]$

R3) Rate of GEF mediated nucleotide exchange =

$$\frac{[GEF](\frac{k_{cat,GDP}}{K_{M,GDP}}[Ras_{GDP}] - \frac{k_{cat,GTP}}{K_{M,GTP}}[Ras_{GTP}])}{1 + \frac{[Ras_{GDP}]}{K_{M,GDP}} + \frac{[Ras_{GTP}]}{K_{M,GTP}}}$$

R4) Rate of Ras GTPase activity = $k_{hyd}[Ras_{GTP}]$

R5) Rate of GAP mediated GTP hydrolysis = $\frac{[GAP]k_{cat}[Ras_{GTP}]}{K_M + [Ras_{GTP}]}$

R6) Rate of Ras, Effector Interaction =

$k_{a,Eff}[Ras_{GTP}][Effector] - k_{d,Eff}[Ras_{GTP}.Effector]$

R7) Rate of Ras GTPase activity in Effector-Ras complex = $k_{hyd}[Ras_{GTP}.Effector]$

These reaction definitions were used to describe the model with ordinary differential equations by grouping all reactions involving each quantity considered.

$$\frac{d[Ras_{GTP}]}{dt} = \text{- (R2) + (R3) - (R4) - (R5) - (R6)}$$

$$\frac{d[Ras_{GDP}]}{dt} = \text{- (R1) - (R3) + (R4) + (R5) + (R7)}$$

$$\frac{d[Ras_{nt\ free}]}{dt} = \text{(R1) + (R2)}$$

$$\frac{d[Effector]}{dt} = \text{- (R6) + (R7)}$$

$$\frac{d[Ras_{GTP}.Effector]}{dt} = \text{(R6) – (R7)}$$

The following conservation relationships were used to check the validity of our code and verify the accuracy of our simulations.

$$Ras_{Total} = Ras_{GTP} + Ras_{GDP} + Ras_{nt\ free} + Ras_{GTP}.Effector$$

$$Effector_{Total} = Effector + Ras_{GTP}.Effector$$

Extension of model to include Ras point mutants

After a spontaneous Ras point mutation, or after exogenous expression of a mutant in a wild-type cell, both mutant and wild-type Ras will be present in the same cell. We extended our model to account for these situations. Except for Reactions 3 and 5 (GEF and GAP catalyzed reactions), the mass-action kinetics descriptions of the mutant reactions are the same as for Ras^{WT}, but with the appropriate parameter values for the mutant used in place of Ras^{WT} values. For reactions 3 and 5, the following equations were used:

R3* A) Rate of GEF mediated nucleotide exchange on Ras^{WT} =

$$\frac{[GEF](\frac{k_{cat,GDP}}{K_{M,GDP}}[Ras_{GDP}] - \frac{k_{cat,GTP}}{K_{M,GTP}}[Ras_{GTP}])}{1 + \frac{[Ras_{GDP}]}{K_{M,GDP}} + \frac{[Ras_{GTP}]}{K_{M,GTP}} + \frac{[Ras^{mut}_{GDP}]}{K_{M,GDP,mut}} + \frac{[Ras^{mut}_{GTP}]}{K_{M,GTP,mut}}}$$

R3* B) Rate of GEF mediated nucleotide exchange on Ras^{mut} =

$$\frac{[GEF](\frac{k_{cat,GDP,mut}}{K_{M,GDP,mut}}[Ras^{mut}_{GDP}] - \frac{k_{cat,GTP,mut}}{K_{M,GTP,mut}}[Ras^{mut}_{GTP}])}{1 + \frac{[Ras_{GDP}]}{K_{M,GDP}} + \frac{[Ras_{GTP}]}{K_{M,GTP}} + \frac{[Ras^{mut}_{GDP}]}{K_{M,GDP,mut}} + \frac{[Ras^{mut}_{GTP}]}{K_{M,GTP,mut}}}$$

R5*A) Rate of GAP catalyzed Ras^{WT} GTP hydrolysis=

$$\frac{[GAP]k_{cat}[Ras_{GTP}]}{K_M(1 + \frac{Ras^{mut}_{GTP}}{K_{M,mut}}) + [Ras_{GTP}]}$$

R5*B) Rate of GAP catalyzed Ras^{mut} GTP hydrolysis=

$$\frac{[GAP]k_{cat,mut}[Ras^{mut}_{GTP}]}{K_{M,mut}(1+\frac{Ras_{GTP}}{K_M})+[Ras^{mut}_{GTP}]}$$

These equations simplify to R3 and R5 when only Ras^{WT} is present. We note that the choice of the $k_{cat,mut}$ parameter dictates that there is no increase in GTP hydrolysis for the GAP-Ras^{mut} complex when Ras^{mut} is a GAP-insensitive Ras mutant (e.g., Ras^{G12V}). Differential equations are created as before, but extended to include terms for both Ras^{WT} and Ras^{mut}.

Parameters

All needed model parameters for Ras^{WT} were found in the literature (table S1). We chose the most recent measurement when multiple measurements were available. Most published measurements have been made on H-Ras. We chose H-Ras when measurements on multiple Ras isoforms were available for the sake of consistency. We note that values for H-, K-, and N-Ras are similar in studies where measurements were made on each of the three isoforms *(S2, S3)*.

There are multiple GAPs and GEFs capable of acting on Ras, and also multiple downstream effectors capable of interacting with Ras. However, there is uncertainty as to which GAPs and GEFs are responsible for the basal activity observed and also uncertainty in the list of proteins which are possible Ras effectors. Therefore, our model does not distinguish between the different GAPs, GEFs, and effectors, and instead groups basally active GAPs, basally active GEFs, and effectors. We then chose parameter values from one representative GAP, GEF, and effector to use in our model. For the GAP, we chose the parameters of NF1 as this is basally active in several cell types as suggested by the increased Ras activation at basal, unstimulated conditions in cells deficient for NF1). A NF1 transcript with a possible transmembrane motif is expressed in a wide variety of tissues, suggesting that it may function as a basally active GAP in a large number of tissues *(S4)*. We used reaction constants for the Ras GEF Cdc25 as it is the most completely characterized Ras GEF in terms of parameters needed for our model. We used parameters for the Ras effector Raf since it is perhaps the best studied Raf effector .

Many of the parameters are related, either by definition (e.g., $K_d = \frac{k_{d,Eff}}{k_{a,Eff}}$) or thermodynamically (e.g., for GEF catalyzed nucleotide exchange and free nucleotide exchange; $(\frac{k_{cat,GDP}K_{M,GTP}}{k_{cat,GTP}K_{M,GDP}} = \frac{k_{d,GDP}\,k_{a,GTP}[GTP]}{k_{d,GTP}\,k_{a,GDP}[GDP]})$. We used these relationships to calculate $k_{cat,GTP}$ and $k_{d,Eff}$.

GAP-insensitive Ras point mutants

The GAP-insensitive Ras point mutants (e.g., Ras^{G12V}) undergo the same reactions as Ras^{WT}, except with different values for the rate constants (e.g., the rate constant for intrinsic GTPase activity of Ras^{G12V} is ~$1/7^{th}$ that of Ras^{WT}). The papers that included the necessary data on Ras^{G12V} and Ras^{G12D} nucleotide exchange and hydrolysis *(S5, S6)* were not the same papers that provided our Ras^{WT} parameters. Additionally, other published values were presented as relative changes in a property compared to wild-type *(S7)*. Therefore, we treat all measurements on mutant Ras as relative changes (compared to the wild-type measurement of the same paper) and applied these relative changes to the more recent Ras^{WT} measurements to model the effects of the mutations (table S2).

As experiments find no measurable change in GTP hydrolysis when a Ras GAP is added to Ras^{G12V} or Ras^{G12D} *(S8)*, we use the rate of hydrolysis for free, mutated Ras as the k_{cat} for the Ras-GAP complex. When we were unable to find published reaction parameters for process involving the Ras^{G12V} and Ras^{G12D} point mutants, we assumed no change (for example, between Ras^{G12D} and effector). Although we found no information regarding changes in association or dissociation rate constants for the Ras^{G12V} interaction with Raf ($k_{a,Eff}$ and $k_{d,\ Eff}$), we found data for the K_d of the interaction. In our calculations, we hold $k_{a,Eff}$ at the Ras^{WT} value and apply the change to $k_{d,Eff}$. Additionally, $k_{cat,GTP}$ was recalculated for the mutants because the other parameter values in the relationship used to calculate this value had changed (Table S2).

Fast-cycling Ras point mutants

Fast-cycling Ras mutants are characterized by an increased rate of spontaneous nucleotide dissociation for both GTP and GDP *(S9-S12)*. We model fast-cycling point mutant Ras^{F28L} with a twenty-five fold increase in $k_{diss,GDP}$ and $k_{diss,GTP}$ *(S13)*. We hold all other properties constant as no significant deviations away from wild-type parameters has been described for F28L GTPase mutant interactions with GAP *(S14)*, GEF *(S15)*, or Effector *(S15)*.

Membrane localization

Post-translational modifications localize Ras to cellular membranes and restrict its reactions to a two-dimensional membrane rather than the three-dimensional cytoplasm. However, rate constants are typically measured in solution. There have been several theoretical papers discussing how membrane localization affects rate constants, including specific mention of the activation of Ras by the GEF Sos *(S16-S18)*. These theoretical treatments suggest methods for adjusting parameters so that they more accurately reflect reactions at the membrane. We use the same technique employed by Markevich et al., in the theoretical study of the kinetics of Ras activation in response to EGFR stimulation, which included comparison of theoretical predictions with experimental time courses *(S19)*. This method involves using a correction factor to adjust second order parameters (such as association rate constants, affinity constants, and Michaelis constants) for reactions between two membrane localized proteins (e.g., Ras with GEF and GAP). We refer to this correction factor as D in Supplementary Table S1.

Concentrations

A recent work that investigated the kinetics of the Ras/MAPK cascade *(S20)* measured the amount of H-, K-, and N-Ras and found the total cellular concentration to be 0.4 μM. Cellular GTP and GDP concentrations have been previously measured in a variety of cell types *(S21)*, we chose the values of 180 μM GTP, 18 μM GDP as they are in the appropriate range and have the widely-mentioned 10× ratio of GTP to GDP in the cell. We keep the concentration of GTP and GDP fixed throughout a simulation.

We next needed to obtain the concentration for total Ras effector proteins. Previous computational studies have typically limited themselves to only one Ras effector (most often, Raf). However, there are many effector proteins known to interact with Ras *(S22)*. Raf, PI3K, and Ral-GDS are perhaps the three most commonly studied. As a Ras-effector interaction will influence the amount of Ras activated, which is the purpose of this study, we need to estimate the total amount of effector concentration in the cell. Microscopic images show little effector at the membrane under basal, unstimulated conditions and a large fraction of effector at the membrane in response to signal or Ras^{G12V} expression *(S23,S24)*. Additionally, experimental evidence suggests downstream behaviors can correspond to the intensity of the Ras signal *(S25)*. We

interpreted this data to mean that the total amount of effector present in the cell is on approximately the same order as the amount of upstream Ras proteins.

Previous experiments have revealed low levels of basal GAP and GEF activity *(S11, S26)* and our model begins at the level of these basally active GAPs and GEFs. With Ras and effector concentrations, we were sufficiently constrained to calculate concentration parameters for the amount of basal GEF and basal GAP present. It should be noted that the concentration of basally active GEF and basally active GAP is not the same as the total concentration of GEF or GAP in the cell, but corresponds only to the fraction of GEF and GAP that is both activated (if its activity is regulated) and in the same location as Ras. We fit the concentration parameter for basally active GEF and GAP using two pieces of previously published experimental data. The first of these studies *(S26)* used permeabilized cells to measure nucleotide exchange under basal, unstimulated conditions *(S27)*. After fifteen minutes, this study found unstimulated cells had reached approximately forty percent of the steady-state exchange level that was reached more quickly under stimulated conditions. The second piece of data that we used is that the fraction of total Ras that is GTP bound under basal, unstimulated conditions tends to be in the range of ~2% *(S28)*. We found the concentration of basally active GEF and basally active GAP that minimized the least-squares percent error for nucleotide exchange at fifteen minutes (40%) and steady-state Ras_{GTP} levels in unstimulated conditions (2%).

Our estimates of the concentration of basally active GAP and GEF is consistent with the Michaelis-Menten assumption that substrate (Ras) is much more abundant that the enzyme(s) acting on it. We also note that these concentrations should not be thought of as corresponding to a measurable concentration, but are rather the effective concentration as if the fraction of basally active GEF and GAP at the membrane were distributed throughout the cytoplasm.

Simulated *in vitro* and *in vivo* conditions

To simulate a mutation *in vivo*, we divide the pool of total cellular Ras between mutant Ras and wild-type Ras. We present the amount of mutated Ras as a percentage of total cellular Ras. When the percentage of cellular Ras mutated is not specified, fifty percent of total Ras is mutated. To simulate exogenous expression of a Ras mutant *in vitro*, mutant Ras is expressed in addition to the pool of cellular wild-type Ras. We present the amount of exogenous Ras as a multiple of the amount of endogenous Ras. When the multiple is not specified, we use 1× of exogenous protein in our simulation.

Computational assessment of Ras signaling

Steady-states were found with simulations in MATLAB 7.1. Ras activation was calculated with two measures. The first of these is the fraction of total Ras bound to GTP (Ras_{GTP}). This measure was useful for comparisons between model predictions and experimental data that measures the fraction or proportion of GTP-bound Ras (e.g. Fig. 1 and Fig. 3). We also use the quantity of total effector protein bound to Ras_{GTP} (Ras-effector) as a measure of Ras activation and often present changes as the total increase (or decrease) in these complexes. Although Ras effectors may still be activated after dissociating from Ras *(S24)*, this other measure of Ras activation should better reflect the extent of downstream signaling (e.g. Fig. 2). This measure is particularly relevant when different drug targeting strategies are considered (Fig. 4) because some drugs (e.g., drugs that interact with Ras_{GTP}) would be expected to both increase Ras_{GTP} levels (by binding and sequestering Ras_{GTP}) and decrease downstream activation (as sequestered Ras_{GTP} would be unable to interact with downstream effectors). As the ultimate goal

of such drugs is to block downstream activation, inhibition would be best characterized by resultant changes in Ras-effector interactions.

Analysis of the contribution of Ras^{G12V} (and Ras^{G12D}) properties

To assess the contribution of each of the Ras point mutant properties on Ras activation, we systematically include properties of the Ras^{G12V} point mutant or replace the property with the corresponding Ras^{WT} parameter value. The nucleotide exchange properties of Ras^{G12V} are inactivating compared to Ras^{WT}. All described mutants, including those with only a partial subset of the altered properties, include the altered nucleotide exchange properties. In the cases where we wanted to remove competitive inhibition from the model, a distinct irreversible Michaelis-Menten equation was used to describe each GAP activity (e.g., on Ras^{WT} and on Ras^{G12V}), to prevent Ras^{G12V} from competitively inhibiting GAP activity on Ras^{WT}.

Dose dependent inhibition by dominant negative Ras^{S17N}

Dominant negative Ras proteins (e.g., Ras^{S17N}) are believed to exert their effect by forming high affinity complexes with Ras GEFs, thus preventing the GEFs from being able to activate Ras *(S29)*. To study the dose dependent effect of Ras^{S17N}, we first calculated the amount of basal GEF not bound to Ras^{S17N} and then ran the simulation with this concentration.

Concentration of free basal GEF =

$$\frac{1}{2}\left([GEF]-K_{d,S17N}-[Ras^{S17N}]+\sqrt{-4[Ras^{S17N}][GEF]+\left([Ras^{S17N}]+[GEF]+K_{d,S17N}\right)^2}\right)$$

Drug interactions

To study the effects of hypothetical drugs A, B, and C, we extended our module to include the appropriate drug (fig. S5) and describe with mass-action kinetics:

R A) Rate of Drug A reaction with $Ras_{GDP} = k_{a,drugA}[Ras_{GDP}][A] - k_{d,drugA}[Ras_{GDP}.A]$

R B) Rate of Drug B reaction with $Ras_{GTP} = k_{a,drugB}[Ras_{GTP}][B] - k_{d,drugB}[Ras_{GTP}.B]$

R C) Rate of Drug C reaction with Ras_{GDP} and Ras_{GTP} =

$$k_{a,drugC}[Ras_{GTP}][C] - k_{d,drugC}[Ras_{GDP}.C] + k_{a,drugC}[Ras_{GTP}][C] - k_{d,drugC}[Ras_{GTP}.C]$$

Each drug binds Ras^{WT} and Ras^{G12V} with identical properties (e.g., $k_{a,drugA}$ and $k_{d,drugA}$ are identical for the Drug A interactions with Ras^{WT}_{GDP} and Ras^{G12V}_{GDP}. We extend the differential equations to include the relevant reactions. We set $k_{a,drug}$ to be 10^7/Ms for all drugs so that it was on the same order as other bimolecular reactions involving Ras, e.g., the Raf-Ras interaction with a $k_{a,Eff}$ of 4.5×10^7/Ms *(S30)*. The dissociation rate constant was calculated using the K_d specified for each simulation. Ras_{GTP} is modeled to retain its GTPase activity when bound Drug B and Drug C. Ras_{GTP}-Drug B, Ras_{GTP}-Drug C, and Ras_{GTP}-Effector GTP hydrolysis is not drawn on fig. S5 for clarity.

Drug assessment

The unregulated (e.g. stimulation independent) activation of Ras in cells that contain oncogenic Ras mutants seems to be the most important consequence of the mutation with regards to transformation potential. In a non-cancerous cell, the ability of Ras to activate in response to a signal seems to be more important for normal cellular function than basal activation levels. To assess the drug's ability to reduce signaling in a cancerous cell, we study our model in the $Ras^{G12V/WT}$ state under unstimulated, basal conditions. To assess the effect of the drug on non-

cancerous cells, we study our model in the $Ras^{WT/WT}$ state under stimulated conditions. For both cases, we find the steady-state concentration of Ras-effector complex. Activation of the Ras signaling module occurs through the recruitment of GEFs to the membrane *(S31)*. To model stimulation, we returned to experimental data of nucleotide exchange on stimulated and non-stimulated cells *(S26)*. Increasing the effective concentration parameter for GEF in our model ten fold to 2×10^{-9} M resulted in a close match with the experimental data *(S26)*. Within the cell, Ras activation in response to a signal is transient; however, our model does not include the many mechanisms that result in the transient signal (e.g., receptor internalization, negative feedback loops). We therefore calculate the steady-state amount of Ras-effector complexes when GEF levels are elevated to assess how the drug affects Ras activation in the $Ras^{WT/WT}$ module.

II. SUPPLEMENTARY TEXT:

Robustness with respect to protein concentrations

As concentrations of proteins likely vary between different cell types, we wanted to investigate the sensitivity of our results to alternative sets of protein concentrations. Toward this, we also considered effector concentrations twice as large and half as large as the concentration of Ras. Furthermore, we considered concentrations of Ras that were twice as large and half as large as the 0.4 μM concentration reported in the literature and used in our primary set of concentrations (table S1). We obtained a GEF and GAP calculation for each set of Ras and effector concentrations as before (complete set of concentrations available in table S3). These are used to assess the robustness of model predictions to alternative sets of protein concentrations (Fig. 1B, 1C and 3B; fig S1, S3, S4, and S6). All error bars on these figures represent the mean +/- SD for simulations results from the nine sets of protein concentration. We find that the results presented in the manuscript are robust and not affected by the set of basal protein concentrations used.

Neurofibromatosis predictions

To test of our model, we also considered a $Ras^{WT/WT}$ network that has lost all basal GAP activity to evaluate the loss of the Ras GAP neurofibromin (NF1) that occurs in the neurofibromatosis disease state. Experimental measurements in NF1(-/-) cells show ~30-50% of total Ras as Ras_{GTP} *(S28)*. Due to the continued expression of other Ras GAPs in these cell *(S28)*, it is not possible to precisely calculate the amount of activated Ras in NF1(-/-) cells with our model. However, the upper bound calculated by eliminating all basal GAP activity in our model (~ 60% of total Ras as Ras_{GTP}) correlates well with the experimental data (table S3).

Correlation between sensitive parameters and disease

The sensitivity analysis in Figure 2A identified four parameters for which an order of magnitude increase or decrease in the parameter resulted in an order of magnitude increase in Ras activation (steady-state Ras-effector complex concentration). For each of these four parameters, a corresponding biological example of how alterations in this parameter are used to trigger physiological Ras activation and/or result in pathological Ras activation exists. We are not aware of any diseases or transforming mutants that result from mutation of reaction parameters that were not found by this analysis.

The k_{cat} (the catalytic constant for GAP activity on Ras_{GTP}) is reduced in GAP-insensitive Ras mutants have *in vitro* transformation potential *(S32)* and are found in human cancers *(S33)*. GAP point mutants have been described in human tumors *(S34)*. The rate constant for spontaneous dissociation of GDP from Ras_{GDP} ($k_{d,GDP}$)is increased in fast-cycling mutants. Fast-cycling Ras mutants have *in vitro* transformation potential *(S9, S10)*, but no natural point mutants have been found in human cancers; however, fast-cycling insertion mutants have been found in human cancers *(S11, S12)*. GEF recruitment/activation is the most common physiological method of Ras activation *(S35)*. In cancer, activation of Ras/MAPK is commonly initiated with upstream mutations that cause GEF activation, e.g., EGFR mutants *(S36)*. The sensitivity analysis predicted that Ras activation is sensitive to two properties of the GEF-Ras interaction: $k_{cat,GDP}$, the catalytic constant for GEF on $Ras_{GDP,}$ and $K_{m,GDP}$, the Michaelis constant for GEF on Ras_{GDP}. To our knowledge, no Ras mutations have been describe with these properties altered. However, germ-line Sos mutations that display increased Ras activation have been described in developmental disorders *(S37, S38)*. It is possible that these Sos mutants have altered $k_{cat,GDP}$ and

$K_{m,GDP}$, however, these mutants remain to be characterized at the level of detail needed to compare with our model.

III. SUPPLEMENTARY FIGURES:

Fig. S1: Robustness of the prediction that GAP-insensitive Ras^{G12V} mutations cause a greater increase in Ras activation (steady-state concentration of Ras-effector complex) to changes in protein concentration. We considered the same sets of in vivo and in vitro conditions as in Fig. 2B for the nine sets of protein concentrations. The value plotted on the y-axis is the increase in Ras-effector concentration caused by the G12V mutant divided by the increase in Ras-effector concentration caused by the F28L mutant. Data are mean +/- SD.

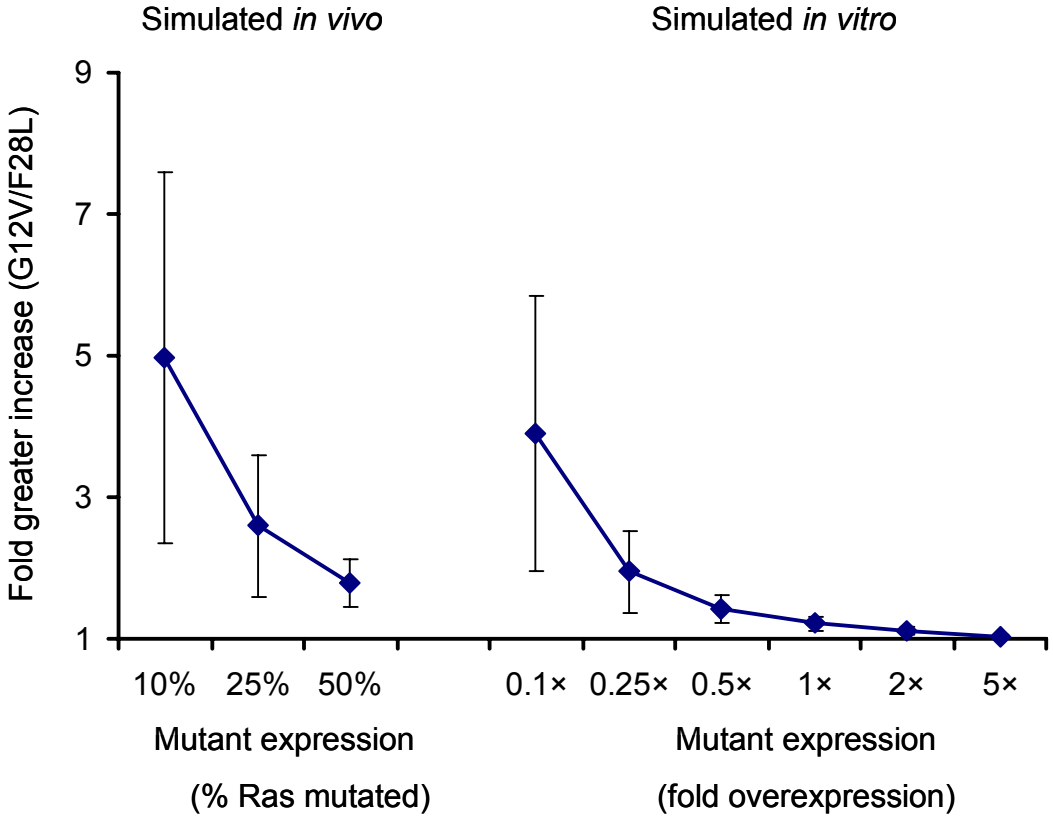

Fig. S2: Flow cytometry based single-cell, quantitative assessment of fast-cycling (F28L) and GAP-insensitive (G12V) Ras mutant-dependent Ras/MAPK pathway activation. Four different plasmid concentrations were used to transiently transfect HA-tagged Ras mutants (G12V or F28L) into HEK293T cells. Ras pathway activation and protein expression were quantified using pERK and anti-HA antibodies, followed by two-color flow cytometry. 50,000 points from the 6 µg DNA condition are used in Figure 2C. Six micrograms of pcDNA3.1 vector plasmid was used as a control.

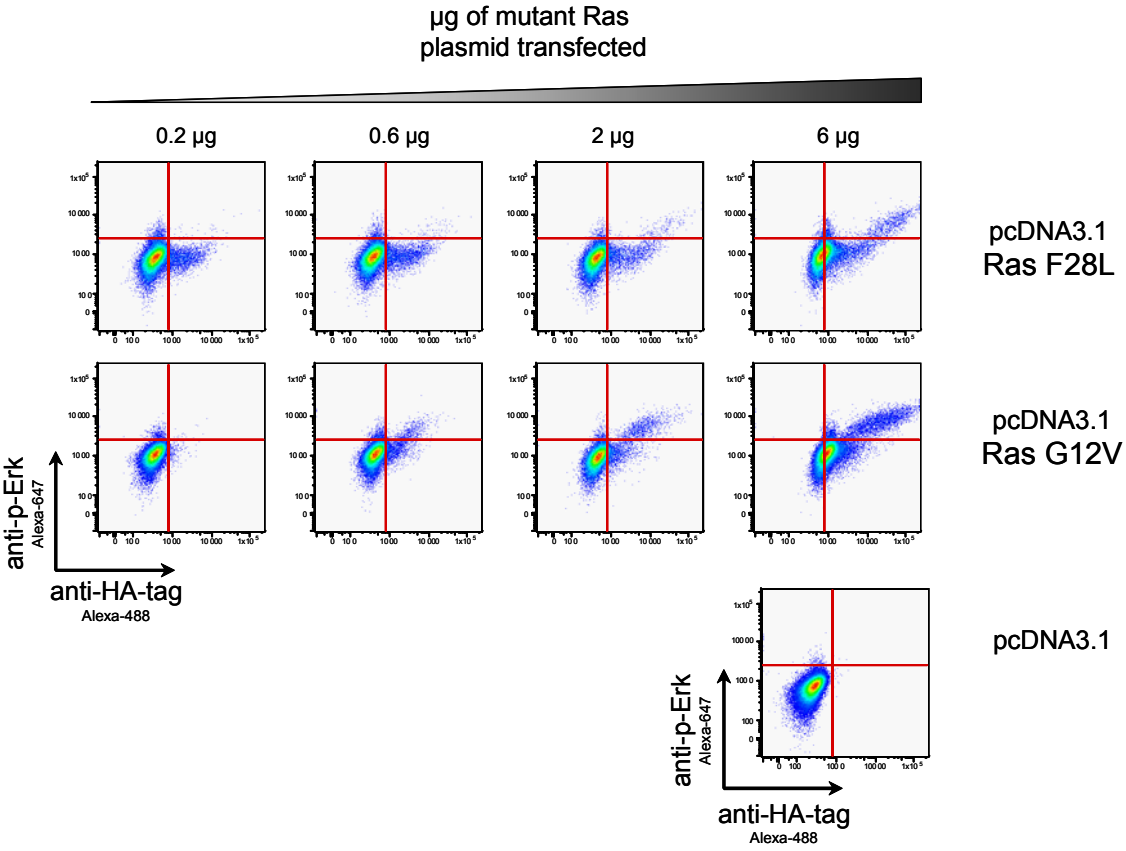

Fig. S3: Robustness of the predicted effects of the multiple biochemical changes in the Ras^{G12V} point mutant on Ras activation. Same analysis as in Fig. 3A except, except done with the nine sets of alternative protein concentrations. The effect of changes in basal GAP concentration was also investigated. (Top) Results for the nine sets of protein concentrations with twice as much GAP in each. (Middle) Results for the standard nine sets of protein concentrations. (Bottom) Results for the nine sets of protein concentrations with half as much GAP in each. Data are mean +/- SD.

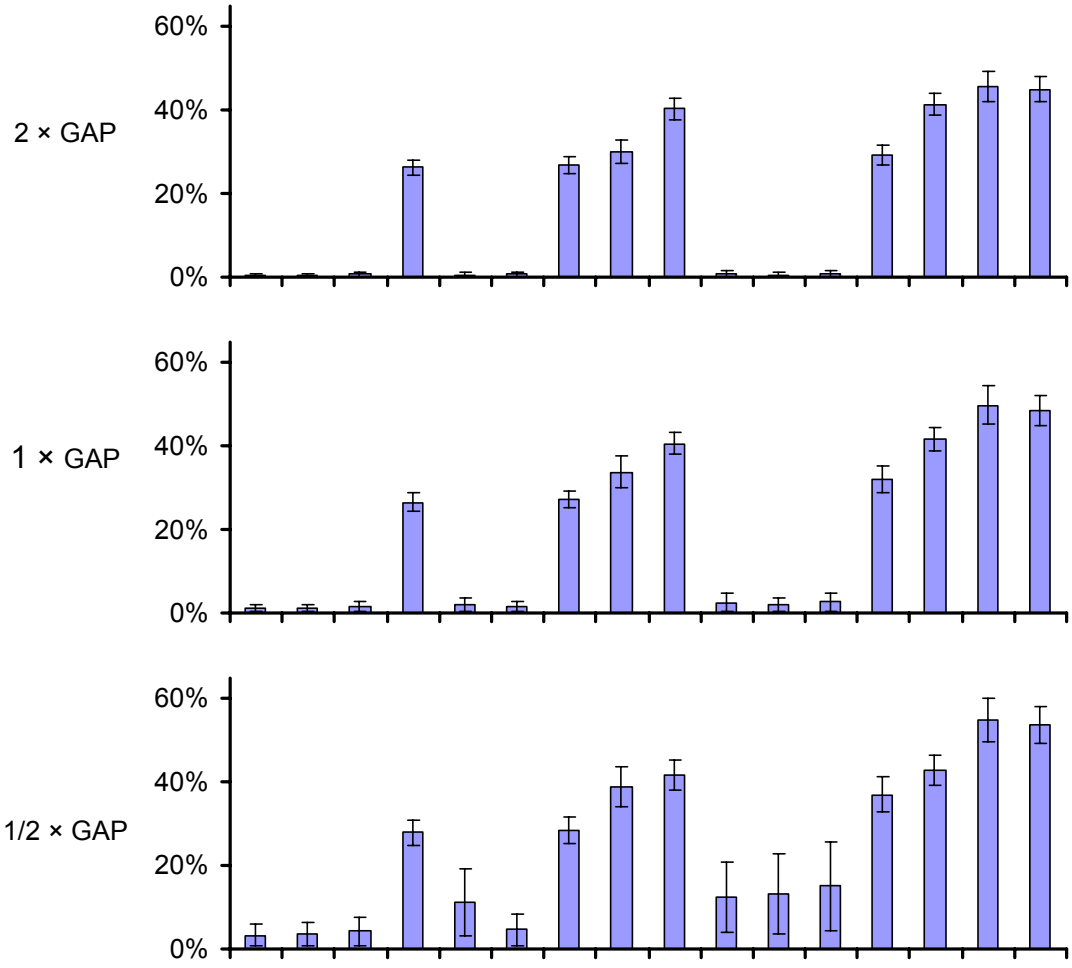

	1	2	3	4	5	6	7	8	9	10	11	12	13	14	15	16
Reduced GTPase activity		+				+			+		+	+		+	+	+
Increased effector affinity			+			+	+			+		+	+	+		+
GAP insensitivity				+			+	+	+				+	+	+	+
Competitive inhibition					+			+		+	+	+	+		+	+

Fig. S4: Robustness of dose-dependent decrease in Ras activation (concentration of Ras-effector complex formation) caused by dominant-negative Ras^{S17N} for both $Ras^{WT/WT}$ and $Ras^{G12V/WT}$ networks. Same analysis as in Fig. 3A except, except done for nine sets of alternative protein concentrations. Data are mean +/- SD.

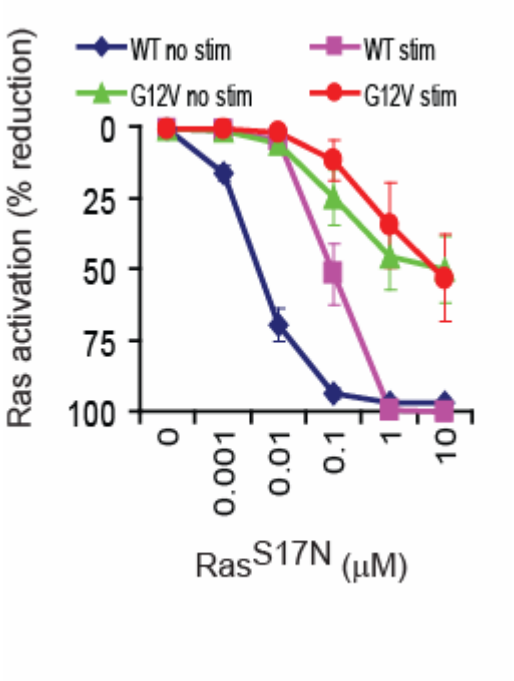

Fig S5: Mechanism of interaction for three potential drug strategies on the Ras module. The diagram does not distinguish, but Ras could be either Ras^{WT} or Ras^{G12V}. Drugs are considered to interact with Ras^{WT} and Ras^{G12V} with identical properties, although each drug interacts with Ras in a nucleotide dependent manner as indicated. Ras_{GTP}-Drug B, Ras_{GTP}-Drug C, and Ras_{GTP}-Effector GTP hydrolysis is not drawn for clarity.

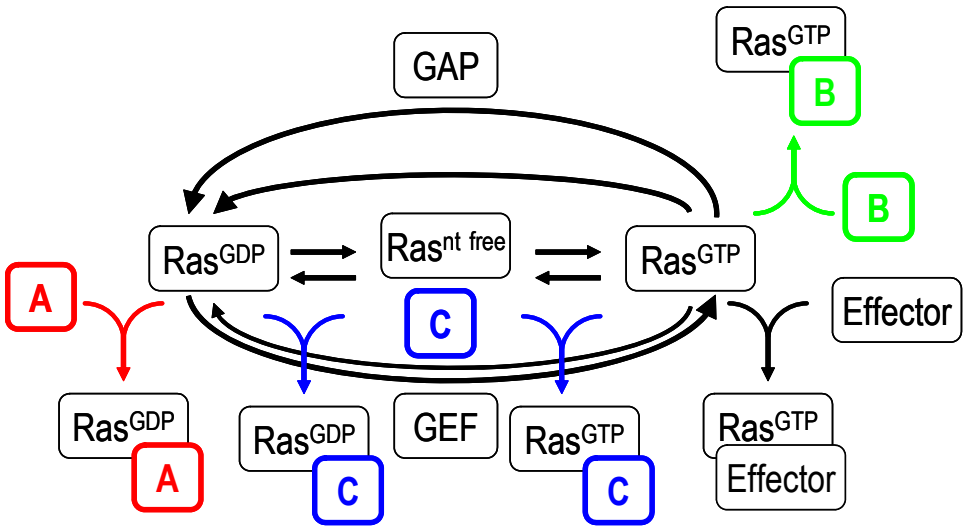

Fig S6: Robustness of the predicted reduction in Ras activation for the three drug strategies. (top) The three drug strategies on the $Ras^{G12V/WT}$ module versus the stimulated $Ras^{WT/WT}$ module (as in Fig. 4B). (bottom) The three drug strategies on the $Ras^{WT/WT}$ module expressing exogenous Ras^{G12V} versus the stimulated $Ras^{WT/WT}$ module (as in Fig. 4D). (top and bottom) 1620 points (9 sets of protein concentrations, 180 different drug conditions for each protein concentration) for each of the three strategies. Drug A, red; Drug B, green; Drug C, blue.

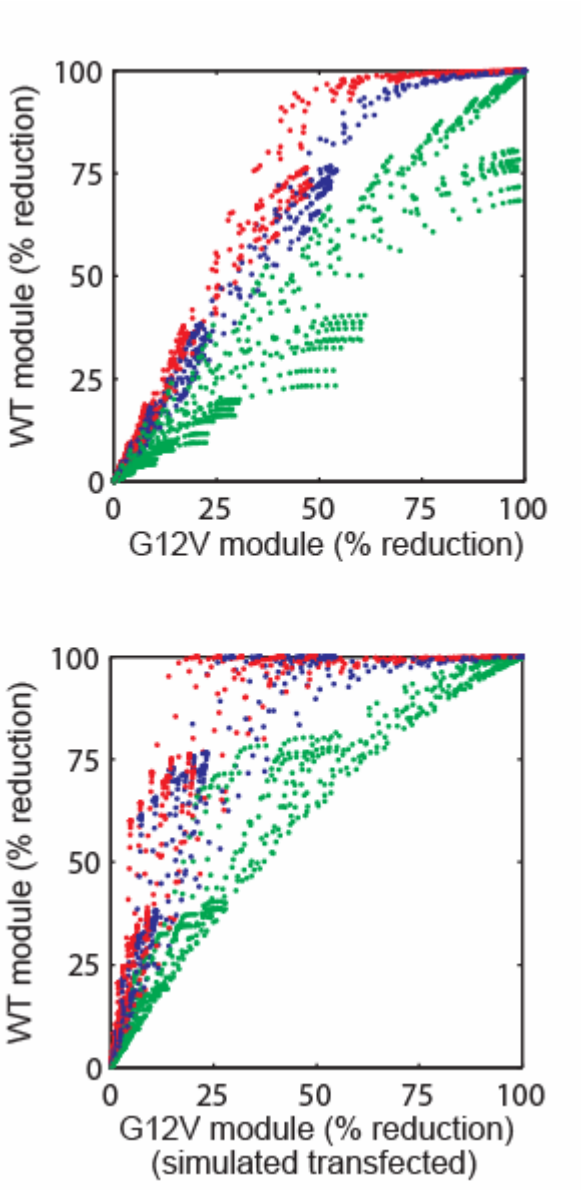

Fig. S7: Steady-state behavior of Ras^{G12V} in the $Ras^{G12V/WT}$ module including Drug B for the different drug concentrations and affinities studied. **(A)** The percentage of free Ras_{GTP} that is comprised of Ras^{G12V}. **(B)** The percentage of complex between Drug B and Ras complex that is comprised of Ras^{G12V}. **(C)** The percentage of Ras-effector complex that is Ras^{G12V}. **(D)** The percentage of total Ras^{G12V} that is bound to Drug B.

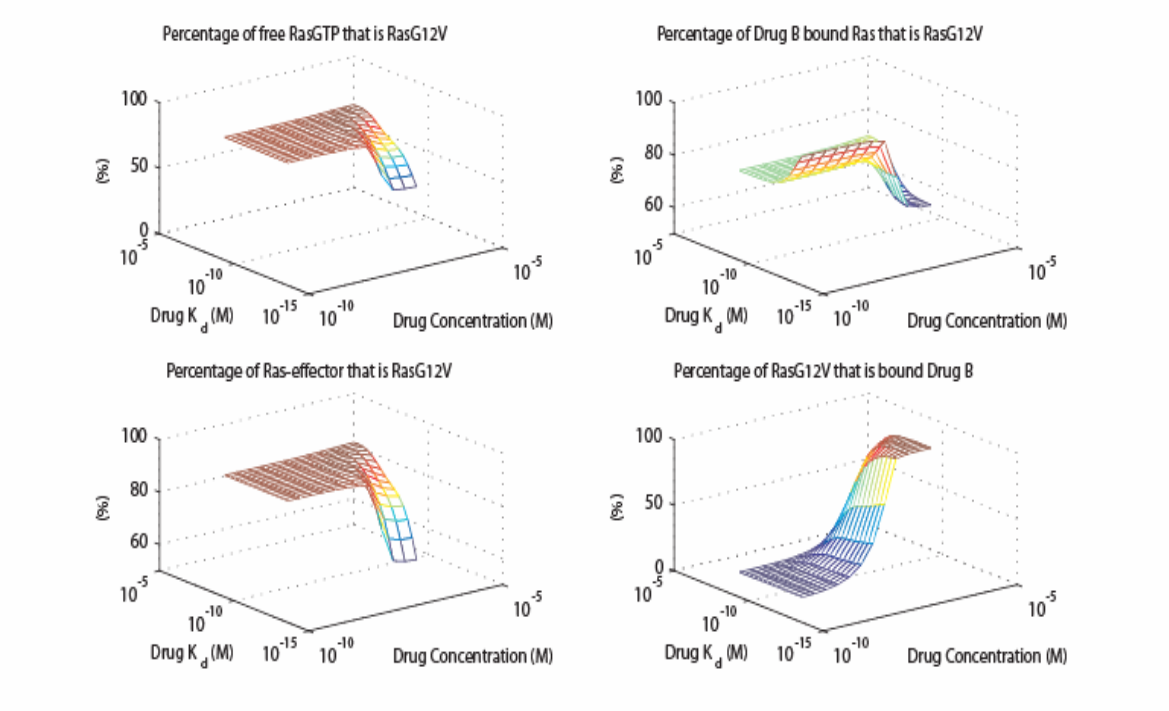

IV. SUPPLEMENTARY TABLES:

Table S1: Properties of the Ras^{WT} signaling module used in our modeling. All of the reaction parameters were taken from published sources or calculated from relevant published data. Concentrations that could not be obtained from published sources were fit to published experimental data.

Parameter	Value	Units	Definition	Ref
			Concentrations	
GTP	1.8×10^{-4}	M	Cellular concentration of GTP	*(S21)*
GDP	1.8×10^{-5}	M	Cellular concentration of GDP	*(S21)*
Ras	4×10^{-7}	M	Concentration of Total Ras	*(S20)*
Effector	4×10^{-7}	M	Concentration of Total effectors	*(S39)*
GEF	2×10^{-10}	M	Concentration of Basally Active GEFs	*(S40)*
GAP	6×10^{-11}	M	Concentration of Basally Active GAPs	*(S40)*
			Ras parameters	
$\mathbf{k_{hyd}}$	3.5×10^{-4}	/s	GTP hydrolysis by Ras	*(S41)*
$\mathbf{k_{d,GDP}}$	1.1×10^{-4}	/s	Rate constant for dissociation of GDP from Ras	*(S41)*
$\mathbf{k_{d,GTP}}$	2.5×10^{-4}	/s	Rate constant for dissociation of GTP from Ras	*(S41)*
$\mathbf{k_{a,GDP}}$	2.3×10^{6}	/Ms	Rate constant for association of GDP to Ras	*(S2)*
$\mathbf{k_{a,GTP}}$	2.2×10^{6}	/Ms	Rate constant for association of GTP to Ras	*(S2)*
			GEF parameters	
$\mathbf{k_{cat,GDP}}$	3.9	/s	k_{cat} for Ras_{GDP} to Ras_{GTP} exchange by GEF	*(S2)*
$\mathbf{k_{cat,GTP}}$	7.2×10^{-1}	/s	k_{cat} for Ras_{GTP} to Ras_{GDP} exchange by GEF	*(S42)*
$\mathbf{K_{m,GDP}}$	3.86×10^{-4}	M	K_m for Ras_{GDP} to Ras_{GTP} exchange by GEF	*(S2)*
$\mathbf{K_{m,GTP}}$	3×10^{-4}	M	K_m for Ras_{GTP} to Ras_{GDP} exchange by GEF	*(S2)*
			GAP parameters	
$\mathbf{k_{cat}}$	5.40	/s	k_{cat} for GAP activity on Ras	*(S3)*
$\mathbf{K_m}$	2.3×10^{-7}	M	K_m for GAP on Ras	*(S3)*
			Effector parameters	
$\mathbf{K_d}$	8×10^{-8}	M	K_d for effector Ras interaction	*(S43)*
$\mathbf{k_{a,Eff}}$	4.5×10^{7}	/Ms	Rate constant for association of effector with Ras_{GTP}	*(S30)*
$\mathbf{k_{d,Eff}}$	3.6	/s	Rate constant for dissociation of effector-Ras_{GTP} complex	*(S42)*
			Membrane Localization Parameters	
D	250		Adjustment to account for membrane localization	*(S19)*

Table S2: **Biochemical properties of oncogenic Ras mutants Ras^{G12V} and Ras^{G12D}.** The differences in reaction properties between oncogenic Ras mutants Ras^{G12V} and Ras^{G12D} are expressed as a multiplicative factor to be applied to the Ras^{WT} values from Table S1.

	G12V		G12D	
Parameter	*Factor*	*Reference*	*Factor*	*Reference*
Ras parameters				
k_{hyd}	.39/2.6	*(S5)*	1.04/2.6	*(S5)*
$k_{d,GDP}$	1.3/4.2	*(S5)*	2.0/4.2	*(S5)*
$k_{d,GTP}$	.8/1.0	*(S5)*	5.0/1.0	*(S5)*
$k_{a,GDP}$	1.16/.51	*(S5)*	.7/.51	*(S5)*
$k_{a,GTP}$	5.8/1.4	*(S5)*	4.8/1.4	*(S5)*
GEF parameters				
$k_{cat,GDP}$	no change	*(S44)*	no change	*(S44)*
$k_{cat,GTP}$	(1.022 /s)	*(S45)*	(3.0273 /s)	*(S45)*
$K_{m,GDP}$	no change	*(S44)*	no change	*(S44)*
$K_{m,GTP}$	no change	*(S44)*	no change	*(S44)*
GAP parameters				
k_{cat}	k_{int}	*(S5)*	k_{int}	*(S5)*
K_m	no change	*(S44)*	no change	*(S44)*
Effector Parameters				
K_d	1/2.25	*(S7)*	no change	*(S44)*
$k_{a,Eff}$	no change	*(S44)*	no change	*(S44)*
$k_{d,Eff}$	1/2.25	*(S7)*	no change	*(S44)*

Table S3: **Model predictions for nine different sets of protein concentrations.** The robustness of the model to variations in protein concentrations was investigated by using nine different sets of protein concentrations. Values in the table are the percent of total Ras bound to GTP. WT refers to a cell with no mutations or exogenous protein expression. No GAP refers to a module with all GAP eliminated to simulate the conditions of NF1(-/-). The exogenous protein transfected is indicated. Total refers to the total pool of Ras (endogenous and exogenous) and exogenous refers to only the transfected protein.

						Transfected				
						Ras^{WT}		Ras^{G12V}		Ras^{G12D}
[Ras] (M)	[Effector] (M)	[GEF] (M)	[GAP] (M)	WT	No GAP	Total	Exogenous	Total	Exogenous	Total
4×10^{-7}	2×10^{-7}	2×10^{-10}	6×10^{-11}	1.2	55.9	6.4	6.4	49.8	75.9	37.8
4×10^{-7}	4×10^{-7}	2×10^{-10}	6×10^{-11}	2.0	58.3	7.9	7.9	53.0	82.2	43.1
4×10^{-7}	8×10^{-7}	2×10^{-10}	6×10^{-11}	3.5	60.0	10.0	10.0	55.6	87.0	48.5
2×10^{-7}	1×10^{-7}	2×10^{-10}	4×10^{-11}	1.0	56.4	3.4	3.4	49.2	76.0	36.3
2×10^{-7}	2×10^{-7}	2×10^{-10}	4×10^{-11}	1.6	58.4	4.6	4.6	51.7	81.5	40.5
2×10^{-7}	4×10^{-7}	2×10^{-10}	4×10^{-11}	2.6	60.1	6.5	6.5	53.9	86.3	45.5
8×10^{-7}	4×10^{-7}	2×10^{-10}	1×10^{-10}	1.2	54.4	4.8	4.8	48.4	74.7	37.1
8×10^{-7}	8×10^{-7}	2×10^{-10}	1×10^{-10}	2.0	57.2	6.3	6.3	52.4	82.0	43.3
8×10^{-7}	1.6×10^{-6}	2×10^{-10}	1×10^{-10}	3.6	58.6	8.4	8.4	55.1	86.4	48.5
			Mean	2.1	57.7	6.5	6.5	52.1	81.3	42.3
			Std Dev	0.9	1.9	1.9	1.9	2.4	4.5	4.4

Table S4: Predicted effects of the multiple biochemical consequences of the G12V point mutation on Ras activation alone and in combination. GAP Insensitivity (GI), Reduced GTPase Activity (GR), Increased Effector Affinity (IA), and Competitive Inhibition of Ras GAP by Ras^{G12V} (CI). $Ras^{G12V/WT}$ with four activating effects is the full $Ras^{G12V/WT}$ module with all effects included. All modeled Ras^{G12V} includes Ras^{G12V} nucleotide exchange properties. $Ras^{G12V/WT}$ module modeled as 50% of total Ras as Ras^{G12V} and 50% of total Ras as Ras^{WT}.

Potentially Activating Ras^{G12V} Effects Included	Total Ras bound GTP	Ras^{WT} bound GTP	Ras^{G12V} bound GTP	Ras-effector complex
$Ras^{WT/WT}$				
	2%	2%	N/A	2%
$Ras^{G12V/WT}$ with no activating effects				
	1%	1%	1%	1%
$Ras^{G12V/WT}$ with one activating effect				
GR	1%	1%	1%	1%
IA	2%	1%	2%	1%
GI	28%	1%	54%	22%
CI	2%	2%	2%	1%
$Ras^{G12V/WT}$ with two activating effects				
GR,IA	2%	1%	2%	1%
GI,IA	28%	1%	55%	25%
GI,GR	42%	1%	84%	33%
GI,CI	36%	17%	54%	28%
IA,CI	2%	2%	3%	2%
GR,CI	2%	2%	2%	1%
$Ras^{G12V/WT}$ with three activating effects				
GI,GR,IA	44%	1%	86%	38%
GR,IA,CI	3%	2%	3%	2%
GI,GR,CI	53%	22%	84%	40%
GI,IA,CI	33%	11%	55%	29%
$Ras^{G12V/WT}$ with four activating effects				
GI,GR,IA,CI	51%	15%	86%	43%

Table S5: Predicted effects of the multiple biochemical consequences of the G12D point mutation on Ras activation alone and in combination. GAP Insensitivity (GI), Reduced GTPase Activity (GR), and Competitive Inhibition of Ras GAP by Ras^{G12D} (CI). $Ras^{G12D/WT}$ with three activating effects is the full $Ras^{G12D/WT}$ module with all effects included. All modeled Ras^{G12D} includes Ras^{G12D} nucleotide exchange properties. $Ras^{G12D/WT}$ module modeled as 50% of total Ras as Ras^{G12D} and 50% of total Ras as Ras^{WT}.

Potentially Activating Ras^{G12D} Effects Included	Total Ras bound GTP	Ras^{WT} bound GTP	Ras^{G12D} bound GTP	Ras-effector complex
$Ras^{WT/WT}$				
	2%	2%	N/A	1%
$Ras^{G12D/WT}$ with no activating effects				
	1%	1%	1%	1%
$Ras^{G12D/WT}$ with one activating effect				
GR	1%	1%	1%	1%
GI	26%	1%	51%	21%
CI	2%	2%	2%	2%
$Ras^{G12D/WT}$ with two activating effects				
GI,GR	34%	1%	66%	26%
GI,CI	34%	16%	51%	26%
GR,CI	2%	2%	2%	2%
$Ras^{G12D/WT}$ with three activating effects				
GI,GR,CI	42%	19%	66%	33%

Table S6: Predicted effects of the multiple biochemical consequences of the G12V point mutation on Ras activation alone and in combination when 25% of total Ras is mutated. The analysis is similar to Table S5, except that here the $Ras^{G12V/WT}$ module is modeled with 25% of total Ras as Ras^{G12V} and 75% of total Ras as Ras^{WT}.

Potentially Activating Ras^{G12V} Effects Included	Total Ras bound GTP	Ras^{WT} bound GTP	Ras^{G12V} bound GTP	Ras-effector complex
$Ras^{WT/WT}$				
	2%	2%	N/A	1%
$Ras^{G12V/WT}$ with no activating effects				
	1%	1%	1%	1%
$Ras^{G12V/WT}$ with one activating effect				
GR	1%	2%	1%	1%
IA	2%	2%	2%	1%
GI	15%	1%	54%	12%
CI	2%	2%	2%	2%
$Ras^{G12V/WT}$ with two activating effects				
GR,IA	2%	2%	2%	1%
GI,IA	15%	1%	55%	13%
GI,GR	22%	1%	85%	18%
GI,CI	22%	12%	54%	18%
IA,CI	2%	2%	3%	2%
GR,CI	2%	2%	2%	2%
$Ras^{G12V/WT}$ with three activating effects				
GI,GR,IA	23%	1%	87%	20%
GR,IA,CI	2%	2%	3%	2%
GI,GR,CI	33%	16%	84%	26%
GI,IA,CI	19%	8%	55%	17%
$Ras^{G12V/WT}$ with four activating effects				
GI,GR,IA,CI	30%	11%	87%	26%

Table S7: Predicted effects of the multiple biochemical consequences of the G12D point mutation on Ras activation alone and in combination when 25% of total Ras is mutated. The analysis is similar to Table S6, except that here the $Ras^{G12D/WT}$ module is modeled with 25% of total Ras as Ras^{G12D} and 75% of total Ras as Ras^{WT}.

Potentially Activating Ras^{G12D} Effects Included	Total Ras bound GTP	Ras^{WT} bound GTP	Ras^{G12D} bound GTP	Ras-effector complex
$Ras^{WT/WT}$				
	2%	2%	N/A	2%
$Ras^{G12D/WT}$ with no activating effects				
	1%	2%	1%	1%
$Ras^{G12D/WT}$ with one activating effect				
GR	1%	2%	1%	1%
GI	14%	1%	51%	11%
CI	2%	2%	2%	2%
$Ras^{G12D/WT}$ with two activating effects				
GI,GR	18%	1%	67%	14%
GI,CI	21%	12%	51%	17%
GR,CI	2%	2%	2%	2%
$Ras^{G12D/WT}$ with three activating effects				
GI,GR,CI	27%	14%	67%	21%

V. REFERENCES:

S1. R. J. de, J. L. Bos, *Oncogene* **14**, 623 (1997).
S2. C. Lenzen, R. H. Cool, H. Prinz, J. Kuhlmann, A. Wittinghofer, *Biochemistry* **37**, 7420 (1998).
S3. M. R. Ahmadian, U. Hoffmann, R. S. Goody, A. Wittinghofer, *Biochemistry* **36**, 4535 (1997).
S4. D. Kaufmann *et al.*, *Biochem. Biophys. Res. Commun.* **294**, 496 (2002).
S5. J. F. Eccleston, K. J. Moore, G. G. Brownbridge, M. R. Webb, P. N. Lowe, *Biochem. Soc. Trans.* **19**, 432 (1991).
S6. S. E. Neal, J. F. Eccleston, A. Hall, M. R. Webb, *J. Biol. Chem.* **263**, 19718 (1988).
S7. E. Chuang *et al.*, *Mol. Cell Biol.* **14**, 5318 (1994).
S8. M. Trahey, F. McCormick, *Science* **238**, 542 (1987).
S9. L. A. Feig, G. M. Cooper, *Mol. Cell Biol.* **8**, 2472 (1988).
S10. G. Patel, M. J. MacDonald, R. Khosravi-Far, M. M. Hisaka, C. J. Der, *Oncogene* **7**, 283 (1992).
S11. G. Bollag *et al.*, *J. Biol. Chem.* **271**, 32491 (1996).
S12. B. Klockow, M. R. Ahmadian, C. Block, A. Wittinghofer, *Oncogene* **19**, 5367 (2000).
S13. J. Heo, S. L. Campbell, *J. Biol. Chem.* **280**, 12438 (2005).
S14. J. Reinstein, I. Schlichting, M. Frech, R. S. Goody, A. Wittinghofer, *J. Biol. Chem.* **266**, 17700 (1991).
S15. R. Lin, S. Bagrodia, R. Cerione, D. Manor, *Curr. Biol.* **7**, 794 (1997).
S16. J. M. Haugh, D. A. Lauffenburger, *Biophys. J.* **72**, 2014 (1997).
S17. B. N. Kholodenko, J. B. Hoek, H. V. Westerhoff, *Trends Cell Biol.* **10**, 173 (2000).
S18. B. N. Kholodenko, *J. Exp. Biol.* **206**, 2073 (2003).
S19. N. I. Markevich *et al.*, *Systems Biology* **1**, 104 (2004).
S20. A. Fujioka *et al.*, *J. Biol. Chem.* **281**, 8917 (2006).
S21. T. W. Traut, *Mol. Cell Biochem.* **140**, 1 (1994).
S22. G. A. Repasky, E. J. Chenette, C. J. Der, *Trends Cell Biol.* **14**, 639 (2004).
S23. S. Traverse *et al.*, *Oncogene* **8**, 3175 (1993).
S24. S. J. Leevers, H. F. Paterson, C. J. Marshall, *Nature* **369**, 411 (1994).
S25. J. M. Shields, K. Pruitt, A. McFall, A. Shaub, C. J. Der, *Trends Cell Biol.* **10**, 147 (2000).
S26. L. Buday, J. Downward, *Mol. Cell Biol.* **13**, 1903 (1993).
S27. A. M. de Vries-Smits, d. van, V, J. Downward, J. L. Bos, *Methods Enzymol.* **255**, 156 (1995).
S28. T. N. Basu *et al.*, *Nature* **356**, 713 (1992).
S29. L. A. Feig, *Nat. Cell Biol.* **1**, E25 (1999).
S30. J. R. Sydor, M. Engelhard, A. Wittinghofer, R. S. Goody, C. Herrmann, *Biochemistry* **37**, 14292 (1998).
S31. A. Aronheim *et al.*, *Cell* **78**, 949 (1994).
S32. C. J. Der, T. Finkel, G. M. Cooper, *Cell* **44**, 167 (1986).
S33. J. L. Bos, *Cancer Res.* **49**, 4682 (1989).
S34. Y. Li *et al.*, *Cell* **69**, 275 (1992).
S35. M. S. Boguski, F. McCormick, *Nature* **366**, 643 (1993).
S36. J. Downward, *Nat. Rev. Cancer* **3**, 11 (2003).
S37. M. Tartaglia *et al.*, *Nat. Genet.* **39**, 75 (2007).

S38. A. E. Roberts *et al.*, *Nat. Genet.* **39**, 70 (2007).
S39. Estimated.
S40. Fit to data.
S41. S. Donovan, K. M. Shannon, G. Bollag, *Biochim. Biophys. Acta* **1602**, 23 (2002).
S42. Calculated from other parameters.
S43. M. G. Rudolph *et al.*, *J. Biol. Chem.* **276**, 23914 (2001).
S44. We assume no change as we found no specific data for this property.
S45. Value shown in parentheses is the value used in simulations rather than a scaling factor. Value was calculated from other parameters.